Emerin prevents BAF-mediated aggregation of lamin A on chromosomes in telophase to allow nuclear membrane expansion and nuclear lamina formation

L. Snyers*, R. Löhnert, K. Weipoltshammer, and C. Schöfer
Medical University of Vienna, Center for Anatomy and Cell Biology, Division of Cell and Developmental Biology, Schwarzspanierstrasse 17, 1090 Vienna, Austria

ABSTRACT **Several studies have suggested a role for the LEM-domain protein emerin and the DNA binding factor BAF in nuclear envelope reformation after mitosis, but the exact molecular mechanisms are not understood. Using HeLa cells deficient for emerin or both emerin and lamin A, we show that emerin deficiency induces abnormal aggregation of lamin A at the nuclear periphery in telophase. As a result, nuclear membrane expansion is impaired and BAF accumulates at the core region, the middle part of telophase nuclei. Aggregates do not form when lamin A carries the mutation R435C in the immunoglobulin fold known to prevent interaction of lamin A with BAF suggesting that aggregation is caused by a stabilized association of lamin A with BAF bound to chromosomal DNA. Reintroduction of emerin in the cells prevents formation of lamin A clusters and BAF accumulation at the core region. Therefore emerin is required for the expansion of the nuclear membrane at the core region to enclose the nucleus and for the rapid reformation of the nuclear lamina based on lamin A/C in telophase. Finally, we show that LEM-domain and lumenal domain are required for the targeting of emerin to exert its function at the core region.**

Monitoring Editor
Dennis Discher
University of Pennsylvania

Received: Feb 16, 2022
Revised: Sep 23, 2022
Accepted: Sep 28, 2022

INTRODUCTION

In eukaryotic cells, the genome is separated from the cytoplasm and organelles by a physical barrier, the nuclear envelope, which comprises the nuclear membrane formed by two closely juxtaposed membranes separated by a lumenal space, the nuclear lamina composed of A- and B-type lamins forming a filamentous network underlying the nuclear membrane, and the nuclear pore complexes. In addition, a number of integral and peripheral membrane proteins of the nuclear envelope, some of which are associated with lamins, contribute to the stability of this structure and have various regulatory functions.

Some of these membrane proteins, such as emerin and LAP2, belong to the LEM-domain protein family, which together represent the products of seven genes. LEM-domain proteins of the nuclear envelope have attracted considerable attention since the discovery of mutations in emerin causing X-linked Emery-Dreifuss muscular dystrophy (EDMD) (Berk *et al.*, 2013b; Muchir and Worman, 2019). They link the nuclear membrane and the nuclear lamina by interacting with lamins A/C and B and contribute to the regulation of gene expression at the nuclear periphery (Brachner and Foisner, 2011). Although unified by the presence of the LEM-domain, these proteins can have very different cellular localizations and molecular functions. For example, the LEM-domain protein ANKLE2 associates with the protein phosphatase PP2A and is located in the endoplasmic reticulum (ER) (Asencio *et al.*, 2012).

The LEM-domain is a ~40 amino acid motif that interacts with the 89-kDa barrier-to-autointegration factor (BAF), a conserved metazoan protein forming dimers with two DNA-binding interfaces and one LEM-domain binding site (Cai *et al.*, 2001). BAF binds double-stranded DNA in a sequence-independent manner. BAF is found

This article was published online ahead of print in MBoC in Press (http://www.molbiolcell.org/cgi/doi/10.1091/mbc.E22-01-0007) on October 6, 2022.

*Address correspondence to: L. Snyers (luc.snyers@meduniwien.ac.at).

Abbreviations used: BAF, barrier-to-autointegration factor; EDMD, Emery-Dreifuss muscular dystrophy; ER, endoplasmic reticulum; GFP, green fluorescent protein; IgF, immunoglobulin fold; LAP2, lamina-associated polypeptide 2; LBR, lamin B receptor; LEM, Lap2-emerin-Man1; NBT/BCIP, nitro blue tetrazolium/5-bromo-4-chloro-3-indolyl-phosphate; NLS, nuclear localization signal; PCR, polymerase chain reaction; VRK, vaccinia related kinase.

in the nucleus and in the cytoplasm during interphase and is thought to have regulatory and protective functions (Wiebe and Jamin, 2016; Guey *et al.*, 2020; Sears and Roux, 2020). Recently, BAF has also been shown to be involved in the detection and repair of nuclear membrane ruptures in interphase (Halfmann *et al.*, 2019; Young *et al.*, 2020). BAF is cytoplasmic during mitosis but reassociates almost entirely with chromosomes within minutes after the end of anaphase following its dephosphorylation by the phosphatase PP2A bound to ANKLE2 or by PP4 (Asencio *et al.*, 2012; Zhuang *et al.*, 2014; Snyers *et al.*, 2018). Several studies have sought to attribute a function to this "catastrophic" event at the end of mitosis, for example, the reformation of the nuclear envelope or the prevention of micronucleus formation (Haraguchi *et al.*, 2008; Samwer *et al.*, 2017). Because of the interaction of BAF with the LEM-domain, it is possible that any LEM-domain protein, regardless of its molecular function, is transiently enriched on the surface of chromosomes in telophase, potentially contributing to postmitotic reassembly of the nuclear envelope.

The membrane protein emerin was shown to have several functions in interphase, such as chromatin bridging and control of gene expression at the nuclear periphery, stabilization of the nuclear lamina by binding lamin A, or mechanosensory signal transduction in striated muscle cells (Barton *et al.*, 2015). Emerin has 254 amino acids most of which, about 220 amino acids, are located in the nucleoplasm; this part contains the LEM-domain near the N-terminus, followed by an unstructured (intrinsic disordered) region, which contains binding sites for several interacting proteins, including lamin A, and mediates emerin self-association (Lee *et al.*, 2001; Berk *et al.*, 2014; Yuan and Xue, 2015). The C-terminal part of emerin includes a membrane-associated region and a conserved intraluminal segment containing 11 amino acids. The self-association of emerin proposed in several studies is consistent with a putative involvement in a scaffolding structure at the nuclear envelope, which would be in agreement with the variety of binding partners reported (Berk *et al.*, 2014; Samson *et al.*, 2017). Various studies have addressed the role of emerin in nuclear envelope reformation after mitosis in HeLa cells and other cell types (Dubinska-Magiera *et al.*, 2019; Haraguchi *et al.*, 2000, 2001; Lee *et al.*, 2001). A transient enrichment of emerin, other LEM-domain proteins, BAF, and lamin A in the middle part of the disk-shaped set of chromosomes (hereafter chromosome disks) in telophase was consistently observed and was called the "core" region. This accumulation is distinct from the enrichment of other proteins of the nuclear envelope, such as the lamin B receptor (LBR) or lamin B1, at the extremities of the chromosome disks, the "noncore" region (Haraguchi *et al.*, 2000; Haraguchi *et al.*, 2008; Lu *et al.*, 2011). Localization of emerin or other LEM-domain proteins to the core region requires BAF and a functional LEM-domain (Lee *et al.*, 2001; Gu *et al.*, 2017). However, the signification and function of this transient structure has remained enigmatic and the precise molecular mechanisms underlying the role of emerin, BAF, lamin A, and other LEM-domain proteins, such as LAP2β, in telophase has not yet been elucidated.

In this study, we have suppressed the expression of emerin in HeLa cells or emerin with one of the two other nuclear envelope proteins, lamin A and LAP2β. We have analyzed the consequences of these depletions on nuclear envelope reformation using epifluorescence and confocal live-cell imaging and fluorescently tagged proteins, including BAF and Lamin A. The results of these experiments shed new light on the exact function of emerin in telophase and on the respective contribution of these proteins on postmitotic reassembly of the nuclear envelope.

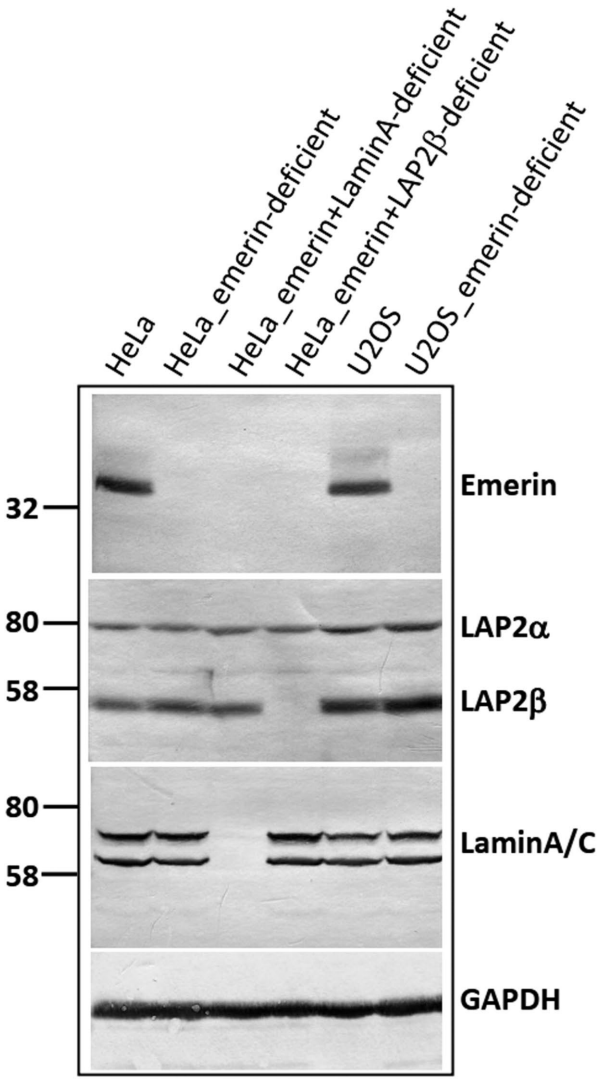

FIGURE 1: Analysis of emerin, lamin A, and LAP2β expression in the cell lines used in this study. Total extracts were resolved by SDS–PAGE and analyzed by immunoblotting using antibodies against emerin, LAP2β, and lamin A. The less abundant membrane isoform LAP2γ is also absent from emerin and LAP2β-deficient cells (not shown).

RESULTS

1. Nuclear membrane closure in telophase is impaired in emerin-deficient cells, inducing a prolonged accumulation of BAF at the core region

To investigate the role of emerin in postmitotic nuclear envelope formation in a cell type amenable to transfection and live microscopy, we generated HeLa cells devoid of emerin using CRISPR/Cas9. Cells were cotransfected with two vectors expressing gRNAs targeting exons 1 and 2 of the emerin gene. After clonal expansion, a cell line was isolated in which the absence of emerin expression was verified by Western blot (Figure 1 and Supplemental Figure S1A) and immunofluorescence (data not shown). These emerin-deficient cells were then stably transfected with GFP-BAF (Supplemental Figure S1, B and C) to observe the redistribution of this protein from early to late telophase in live-cell imaging and compare it with normal cells (Figure 2A and Supplemental Video S1). In both cell types, BAF reassociated rapidly and completely with the chromosomes after the end of anaphase. After 4–6 min, BAF in normal cells became slightly and transiently enriched in the core region and

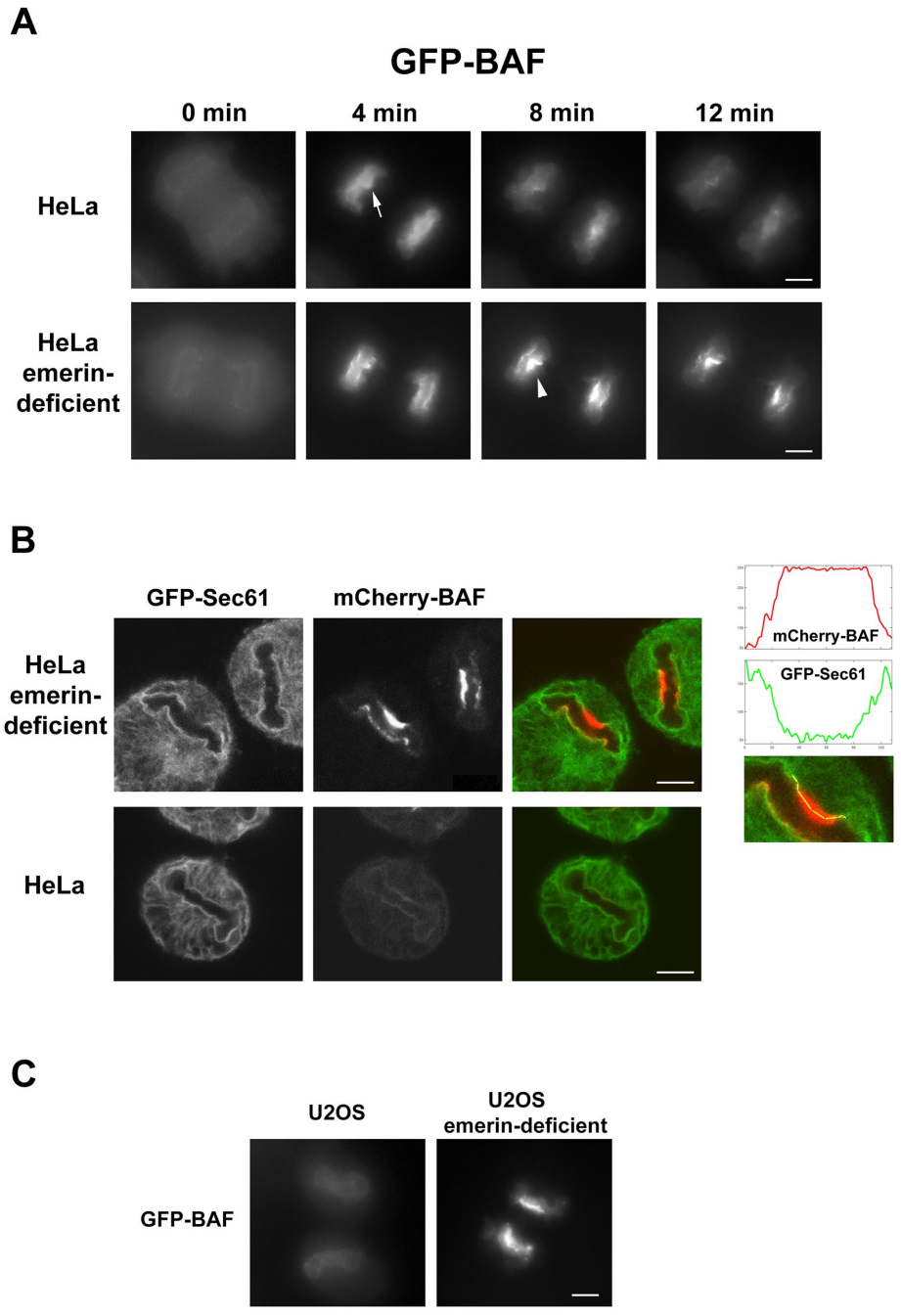

FIGURE 2: GFP-BAF forms a cap on the core region, which is not covered by the nuclear membrane, in emerin-deficient HeLa and U2OS cells. (A) Normal or emerin-deficient HeLa cells stably expressing GFP-BAF imaged at different times after the onset of BAF reassociation with chromosomes using epifluorescence live-cell imaging (Supplemental Video S1). The arrow indicates the transient concentration of BAF at the core region in normal cells and the arrowhead indicates BAF accumulation on the core after 8 min in emerin-deficient cells. For quantification see Figure 5B. (B) Emerin-deficient HeLa cells or normal HeLa cells stably expressing mCherry-BAF were transfected with GFP-Sec61 and imaged in late telophase using confocal live-cell imaging (Supplemental Video S2). Line scan analysis was performed using ImageJ. (C) Normal or emerin-deficient U2OS cells stably expressing GFP-BAF photographed 20 min after the onset of BAF reassociation with chromosomes (Supplemental Video S3). Bars, 5 μm.

then adopted a more homogeneous distribution in the nucleoplasm, the nuclear envelope, and in the cytoplasm. In contrast, in emerin-deficient cells, BAF accumulated progressively after 5 min on the surface of the medial part of the nuclei, eventually forming a conspicuous patch on the core region (more pronounced on the side facing the mitotic spindle). GFP-BAF accumulation reached a maximum between 7 and 10 min after the onset of BAF reassociation with the chromosomes, but then the intensity of the patch gradually decreased until it disappeared completely after 15–20 min (the end of the decreasing part is not shown in Figure 2A and Supplemental Video S1).

The brief concentration of BAF, lamin A, and LEM-domain proteins at the core region in normal cells is thought to correspond to a transient structure involved in nuclear envelope formation (Haraguchi *et al.*, 2008). However, the prolonged accumulation of GFP-BAF on the core region in emerin-deficient cells was reminiscent of the recently reported binding of cytoplasmic BAF at sites of nuclear rupture (Halfmann *et al.*, 2019; Young *et al.*, 2020), suggesting that the core region was not completely covered by the nuclear membrane at the end of telophase in these cells. To explore this possibility, we transfected emerin-deficient cells stably expressing mCherry-BAF with GFP-Sec61 to visualize the nuclear membrane (Lu *et al.*, 2011) and examined cells in late telophase using confocal live-cell imaging (Figure 2B and Supplemental Video S2, first movie). The results clearly show an area on the core region not covered by nuclear membrane in late telophase, which corresponds exactly to the fluorescence spot formed by mCherry-BAF. In contrast, in normal cells expressing mCherry-BAF, the nuclear membrane, labeled with GFP-Sec61, expanded rapidly over the core region to finally enclose the nucleus; as a result, BAF did not accumulate further and was cleared from the core (Figure 2B and Supplemental Video S2, second movie). We conclude that emerin is required to ensure the rapid closure of the nuclear membrane over the core region during the last phase of nuclear envelope reassembly. Note that emerin-deficient cells in interphase were comparable to normal HeLa cells, with respect to nuclear shape and BAF localization, except that BAF was slightly reduced at the nuclear rim, presumably due to a decrease in BAF binding sites (Supplemental Figure S2A). To test whether the absence of emerin could induce the same phenotype in another cell type, we generated U2OS cells devoid of emerin and stably transfected them with GFP-BAF. Figure 2C and Supplemental Video S3 show that GFP-BAF formed a cap on the core region during telophase in emerin-deficient U2OS cells but not in normal cells. Thus the defect in nuclear membrane formation induced by emerin deficiency is not specific to HeLa cells.

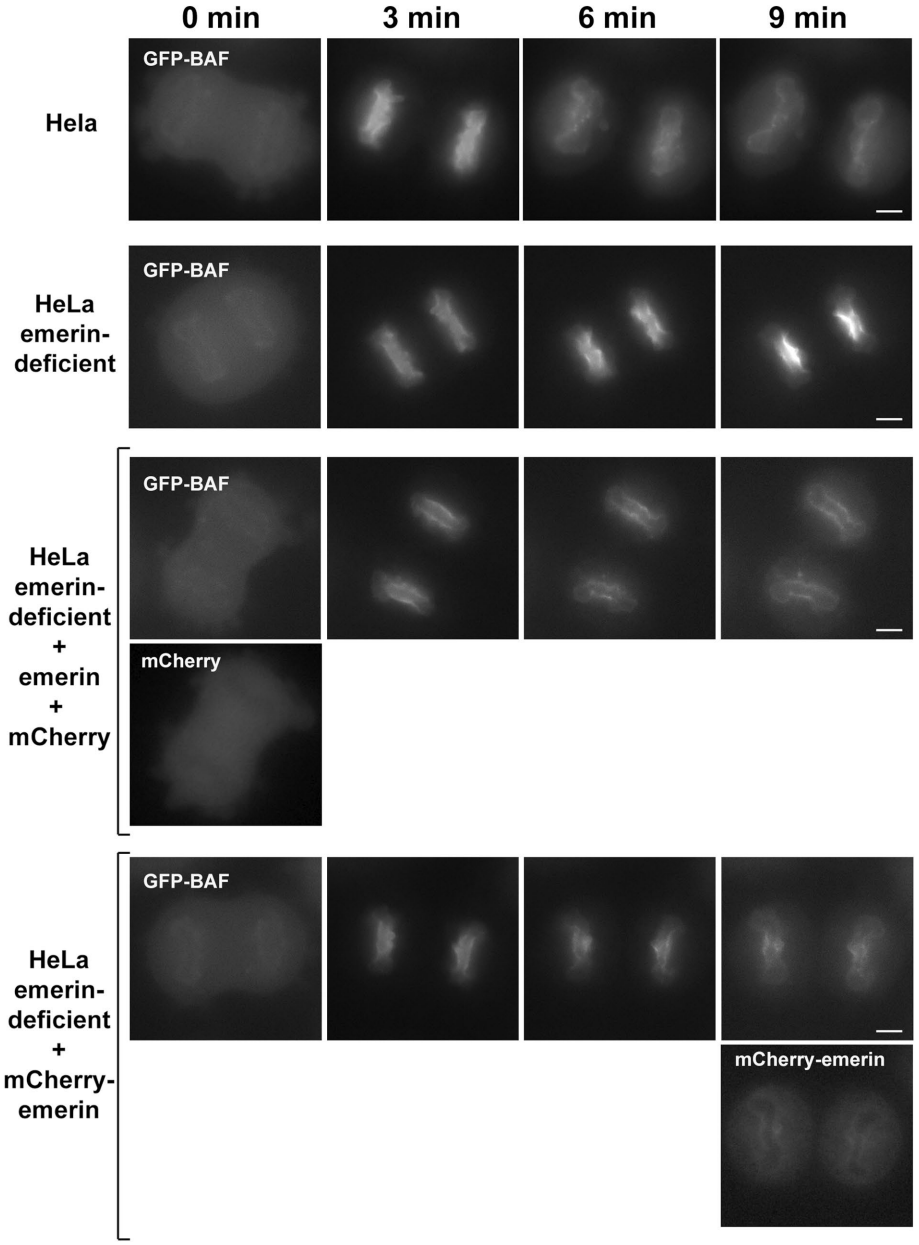

FIGURE 3: Transfection of emerin restores nuclear envelope formation in emerin-deficient cells. Normal or emerin-deficient HeLa cells, stably expressing GFP-BAF, or emerin-deficient cells expressing GFP-BAF transfected with emerin or mCherry-emerin were imaged at different times after the onset of BAF reassociation with chromosomes using live-cell imaging (Supplemental Video S4). Cells expressing untagged emerin were identified by cotransfection of emerin with mCherry (shown under the first image of the third time-lapse sequence). The image under the last panel of the fourth sequence shows mCherry-emerin. Bars, 5 μm.

Then, to confirm that the defect was due to the absence of emerin, we transfected emerin-deficient cells stably expressing GFP-BAF with untagged emerin (and a plasmid expressing mCherry to identify transfected cells) or with emerin fused at its N-terminus to mCherry (mCherry-emerin) and performed live-cell imaging. Figure 3 and Supplemental Video S4 show that GFP-BAF reached a homogeneous distribution in the nuclear envelope and the nucleoplasm within 5 min after reassociation with chromosomes when emerin or mCherry-emerin was transfected in emerin-deficient cells, suggesting that the nuclear envelope formed as rapidly as in normal HeLa cells. Importantly, these cells showed no evidence of BAF accumulation in the core region, indicating that the chromosomes were efficiently isolated from the cytoplasm by the nuclear membrane. We next examined the progression of the nuclear membrane over the core region in emerin-deficient cells transfected with mCherry-emerin and GFP-Sec61 using confocal live-cell imaging. Figure 4 (upper panels) and Supplemental Video S5 (first movie) show that mCherry-emerin readily induced expansion of the nuclear membrane and covering of the core region in the absence of endogenous emerin. The movement of emerin with the nuclear membrane from the noncore to the core region occurred in about 3 min, as in normal cells (Haraguchi *et al.*, 2000), until membrane fusion induced a brief enrichment of emerin at the level of the core. As a negative control for this experiment, we transfected the cells with mCherry-emerin(46-254), which lacks the LEM-domain and thus cannot bind BAF (Figure 4, lower panels, and Supplemental Video S5, second movie). The data show that mCherry-emerin(46-254) was not actively targeted to the nuclear membrane and, unlike full-length mCherry-emerin(1-254), did not induce membrane closure over the core region in emerin-deficient cells. Note that a variety of emerin mutants will be analyzed in detail in Section 3. Finally, to corroborate the different dynamics of core and noncore proteins in our model, emerin-deficient cells were cotransfected with mCherry-emerin and GFP-LBR, showing that the LBR was initially more abundant at the ends of the chromosome disks and was therefore partially and transiently segregated from emerin (Supplemental Video S6). It is also important to note that emerin transiently enriched not only on the side of the core region facing the mitotic spindle but also on the opposite side facing the cytoplasm (see *Discussion*).

2. Aggregation of lamin A prevents nuclear membrane expansion in telophase in emerin-deficient cells

In addition to BAF and LEM-domain proteins, the nuclear envelope protein lamin A is enriched at the core region in telophase in HeLa cells. To analyze the influence of emerin we stably transfected emerin-deficient cells with GFP-lamin A (Supplemental Figure S1D) and examined the redistribution of this protein in telophase using confocal live-cell imaging (Figure 5A and Supplemental Video S7). Similar to BAF, lamin A showed prolonged accumulation at the core region in telophase in emerin-deficient cells, which was short and transient in normal cells or did not occur in emerin-deficient cells transfected with emerin. This observation warranted further investigation of the role/influence of lamin A in emerin-dependent nuclear membrane formation. Therefore we transfected a

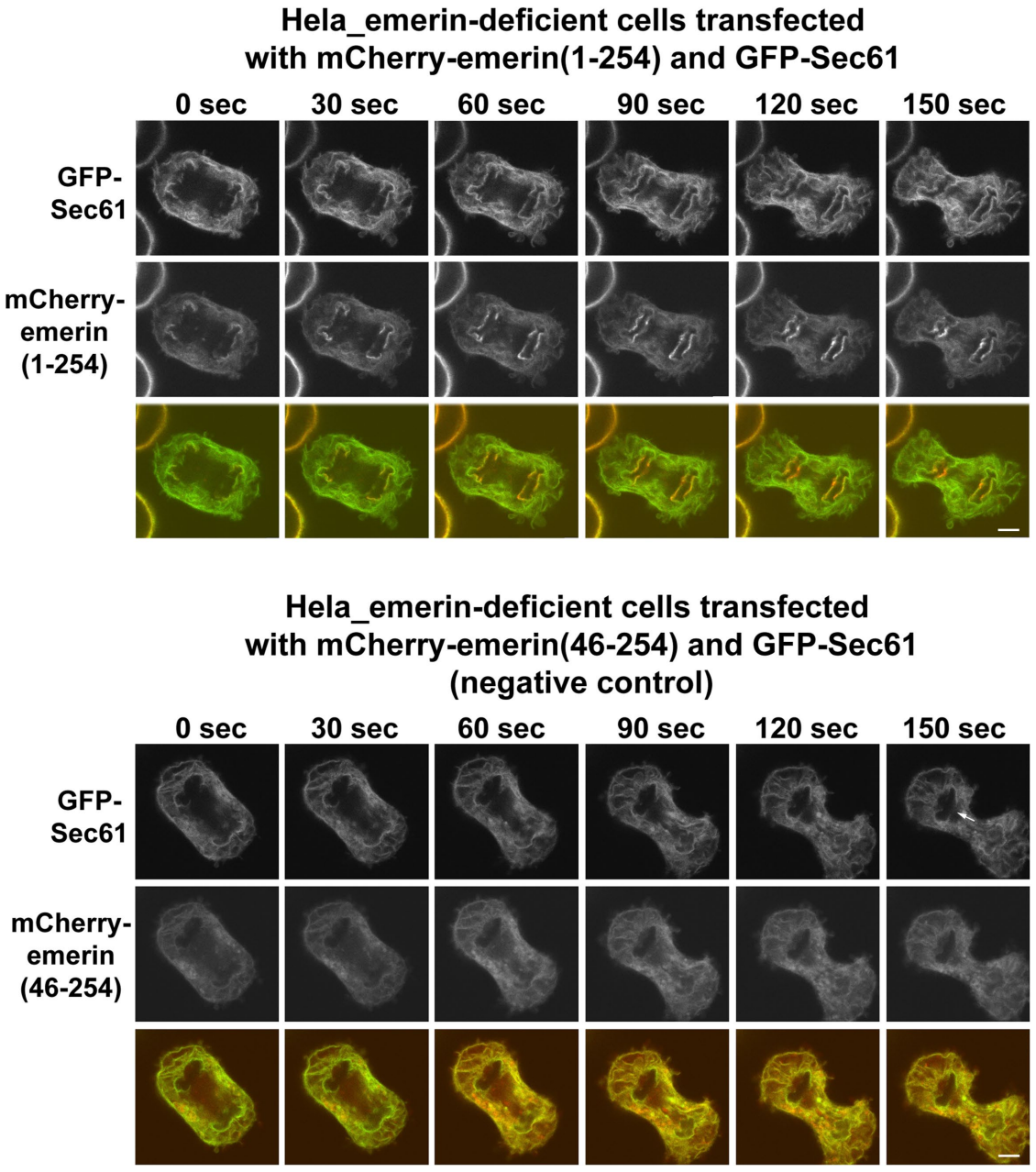

FIGURE 4: Emerin induces the covering of the core region by the nuclear membrane. Upper panels: emerin-deficient HeLa cells transiently transfected with GFP-Sec61 and full-length mCherry-emerin(1-254) imaged at different times after the onset of cytokinesis using confocal live-cell imaging (Supplemental Video S5, first movie). Lower panels: emerin-deficient cells transfected with GFP-Sec61 and mCherry-emerin(46-254), lacking the LEM-domain, as negative control (Supplemental Video S5, second movie). The arrow (GFP-Sec61, 150 s) indicates the area where the nuclear membrane is not closed on the core region. Bars, 5 μm.

CRISPR/Cas9 gRNA targeting exon 1 of lamin A in emerin-deficient cells to generate cells lacking both emerin and lamin A, which were then stably transfected with GFP-BAF (Figure 1 and Supplemental Figure S1); these double-deficient cells were examined in telophase using live-cell imaging (Figure 5B and Supplemental Video S8). Surprisingly, the accumulation of GFP-BAF on the core region observed in emerin-deficient cells did not occur in emerin- and lamin A-deficient cells. BAF enrichment at the core starting 3–4 min after the onset of chromosome binding was readily resolved within 6–8 min in these cells, whereas in emerin-deficient cells, as described above, BAF accumulated on the core region between 6 and 10 min after BAF reassociation. Therefore cells lacking emerin and lamin A were very similar to normal HeLa cells with respect to the spatiotemporal dynamics of BAF in the core region, suggesting that nuclear membrane formation and closure were equally rapid and efficient in both cell types. To verify that the membrane was sealed over the core, emerin- and lamin A-double-deficient cells stably expressing mCherry-BAF were transfected with GFP-sec61 and examined in telophase by confocal live-cell imaging (Figure 5C and Supplemental Video S9). The results show that, in these cells, closure of the gap in the nuclear membrane at the core region occurred rapidly and was followed by the disappearance of mCherry-BAF from the core, in contrast with cells only devoid of emerin.

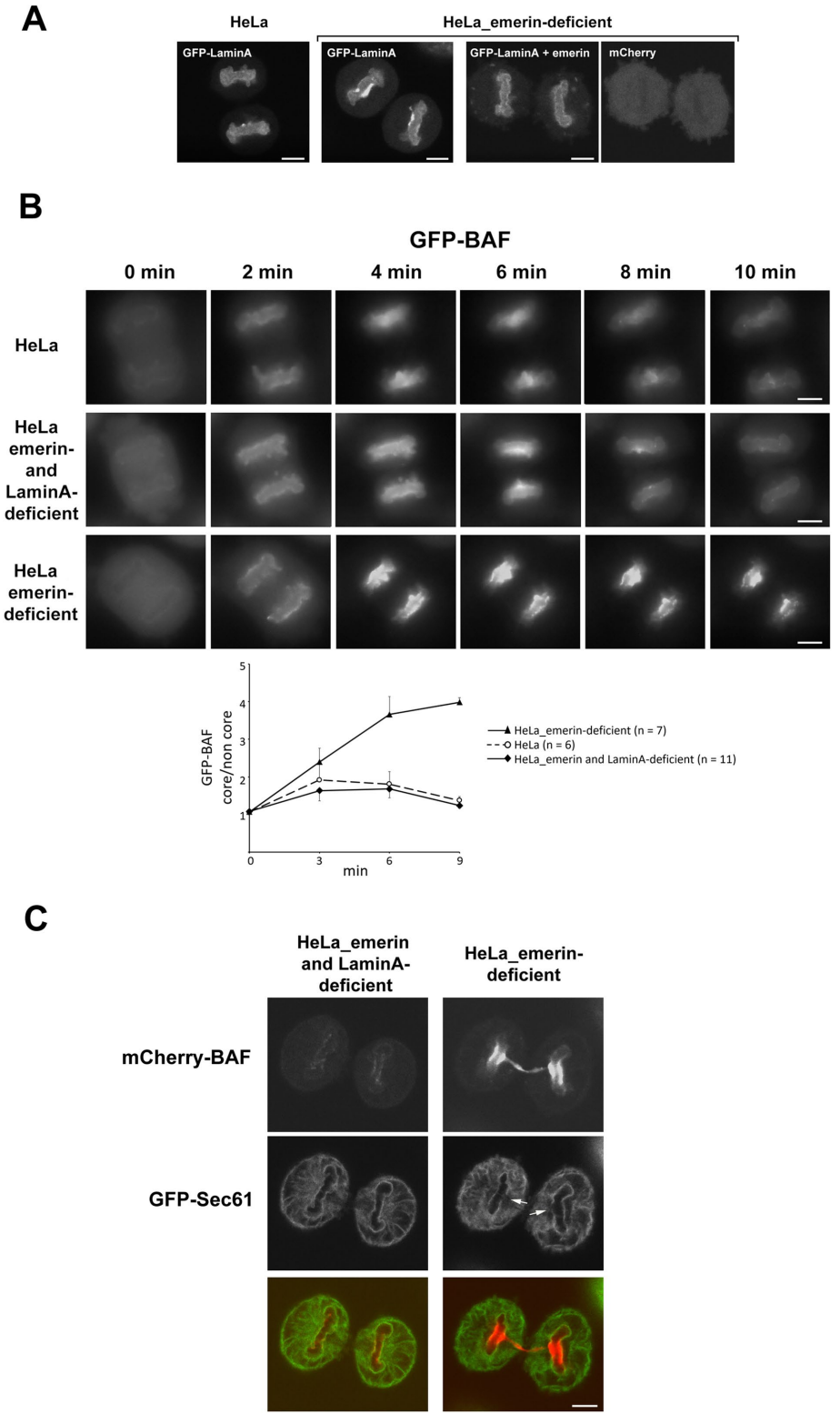

FIGURE 5: GFP-lamin A accumulates at the core region in telophase in emerin-deficient cells and depletion of lamin A restores rapid nuclear membrane formation in emerin-deficient cells. (A) Normal or emerin-deficient HeLa cells stably expressing GFP-lamin A or emerin-deficient cells expressing GFP-lamin A transiently transfected with untagged emerin were imaged 7–8 min after the onset of cytokinesis using confocal live-cell imaging (Supplemental Video S7). Cells transfected with emerin were identified by cotransfection with mCherry (right panel). (B) Normal, emerin-deficient or emerin and lamin A-double-deficient HeLa cells stably expressing GFP-BAF were imaged at different times after the onset of BAF reassociation with chromosomes using epifluorescence live-cell imaging (Supplemental Video S8). In the graph, the average GFP-BAF fluorescence (mean intensity) in the medial region of chromosome disks or at the core region was divided by the average fluorescence in the noncore region at different time points after BAF reassociation with the chromosomes. (C) Emerin-deficient or emerin and lamin A-double-deficient HeLa cells stably expressing mCherry-BAF were transfected with GFP-Sec61 and imaged 8 min after the onset of BAF reassociation with the chromosomes (Supplemental Video S9). The arrows indicate areas of the core region not covered by the nuclear membrane. Bars, 5 μm.

These data indicate that emerin actually becomes dispensable in the last stage of postmitotic nuclear membrane formation when lamin A is not present in the cells. We hypothesized that an interaction between emerin and lamin A might be important for the correct reformation of the nuclear envelope in telophase. Previous reports have shown that some lamin A is enriched at the nuclear periphery at the beginning of telophase, preceding the recruitment of the majority of (cytoplasmic) lamin A to the nucleus interior (Moriuchi *et al.*, 2016; Snyers *et al.*, 2018, see also Supplemental Video S7). To examine whether (and how) this enrichment of lamin A at the periphery of the new nucleus might interfere with nuclear membrane expansion when emerin is absent, we transfected GFP-lamin A in emerin- and lamin A-double-deficient cells stably expressing mCherry-BAF. As shown in Figure 6A and Supplemental Video S10, lamin A progressively accumulated at the periphery of the nucleus during telophase, forming irregular clusters, which then concentrated in the core region; in addition, mCherry-BAF formed a cap on the core region indicating that the nuclear membrane was not closed at this location. As a control, BAF accumulation on the core did not occur when the same cells were transfected with GFP (Figure 6A and Supplemental Video S10). Transfection of emerin- and lamin A-deficient cells with GFP-lamin A and H2B-mCherry showed that lamin A clusters were restricted to the surface of the nuclei (Supplemental Figure S2B). Consistent with these data, detection of lamin A by immunofluorescence revealed sites of endogenous lamin A accumulation at the level of the core region during telophase in (nontransfected) emerin-deficient cells but not in normal Hela cells (Supplemental Figure S2C). Importantly, cotransfection of mCherry-emerin with GFP-lamin A in emerin- and lamin A-deficient cells was sufficient to

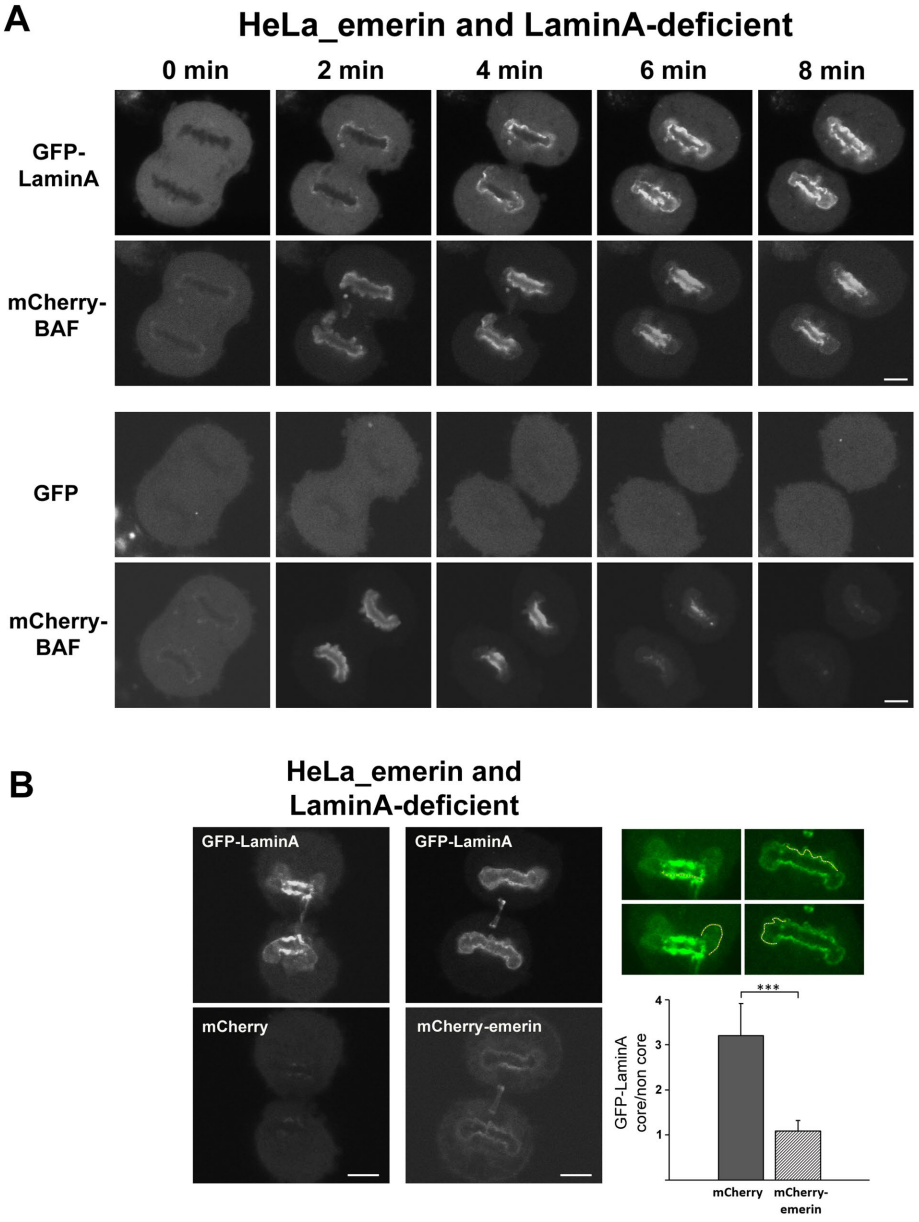

FIGURE 6: In the absence of emerin, lamin A forms aggregates on the surface of telophase chromosomes, which impairs nuclear membrane reformation, and reintroduction of emerin prevents lamin A aggregation. (A) Emerin and lamin A-double-deficient cells stably expressing mCherry-BAF were transfected with GFP-lamin A (upper panels/time-lapse sequence) or with GFP (lower sequence) and observed in telophase at different times after the onset of BAF reassociation with chromosomes using confocal live-cell imaging (Supplemental Video S10). (B) Emerin and lamin A-deficient cells transfected with GFP-lamin A and mCherry (left panels of the grayscale images) or GFP-lamin A and mCherry-emerin (right panels of grayscale images) were imaged in telophase 6–7 min after the onset of cytokinesis using confocal live-cell imaging (Supplemental Video S11). For quantification, mean gray scale value of the line scans corresponding to the surface of the core and noncore regions, as shown in the color images, was determined with ImageJ; the ratios of these values (i.e., core divided by noncore) from several independent experiments are plotted. Error bars correspond to standard deviations (cells transfected with mCherry, dark gray, $n = 17$; with mCherry-emerin, hatched bars, $n = 14$). The ratio is closed to one for cells transfected with mCherry-emerin, indicating a homogeneous distribution of GFP-lamin A in the nuclear rim. Bars, 5 μm.

prevent the formation of lamin A aggregates, demonstrating that emerin directly controls the fate of lamin A at the nuclear envelope in telophase (Figure 6B and Supplemental Video S11).

Since lamin A can bind BAF directly through the immunoglobulin fold (IgF) (Holaska *et al.*, 2003; Samson *et al.*, 2018), we reasoned that the abnormal accumulation of GFP-lamin A on the surface of telophase chromosomes might be induced by the adhesion of lamin A to BAF bound to chromosomal DNA. To answer this question, we transfected emerin- and lamin A-double-deficient cells stably expressing mCherry-BAF with GFP-lamin A containing the restrictive dermopathy mutation R435C, which has been shown to prevent binding of the IgF (comprising R435) to BAF (Samson *et al.*, 2018); these cells were compared with cells transfected with GFP-lamin A containing the autosomal EDMD mutation R453W, which, according to the same study, does not inhibit BAF binding (Figure 7 and Supplemental Video S12). Strikingly, lamin A R435C did not form clusters at the surface of the nuclei, unlike GFP-lamin A R453W, strongly suggesting that aggregation of lamin A is induced by association of the IgF with BAF. In addition, lamin A R453C did not induce BAF accumulation at the core region, indicating that nuclear membrane formation was not impaired by this mutant. Of note, GFP-lamin A, GFP-lamin A R435C, and GFP-lamin A R453W were all localized at the nuclear rim and in the nuclear interior in interphase (data not shown). Confirming that BAF binds to lamin A and not to lamin A R435C, significant enrichment of BAF at the nuclear periphery in interphase was induced by (over)expression of lamin A, but not lamin A R435C, in cells lacking emerin and lamin A, where BAF enrichment at the nuclear rim is otherwise almost nonexistent (Supplemental Figure S2D).

Supplemental Videos S7 and S11 suggest that emerin promotes the rapid formation of a lamin A-containing structure at the periphery of postmitotic nuclei. By comparing emerin- and lamin A-deficient cells transfected with mCherry-emerin and GFP-lamin A with the same cells transfected with mCherry-emerin and GFP-lamin A R435C, it was manifest that the mutation R435C prevents the formation of this structure at the nuclear periphery, even when emerin is present (Supplemental Video S13). Furthermore, we generated HeLa cells lacking only lamin A and, consistently, an initial lamin A/C-based nuclear lamina formed when GFP-lamin A was expressed in these cells but not GFP-lamin A R435C (Supplemental Figure S3A). Therefore we conclude that both the binding of lamin A to BAF via the IgF domain and the presence of emerin are required for the rapid and correct reassembly of the lamin A/C-based nuclear lamina after mitosis.

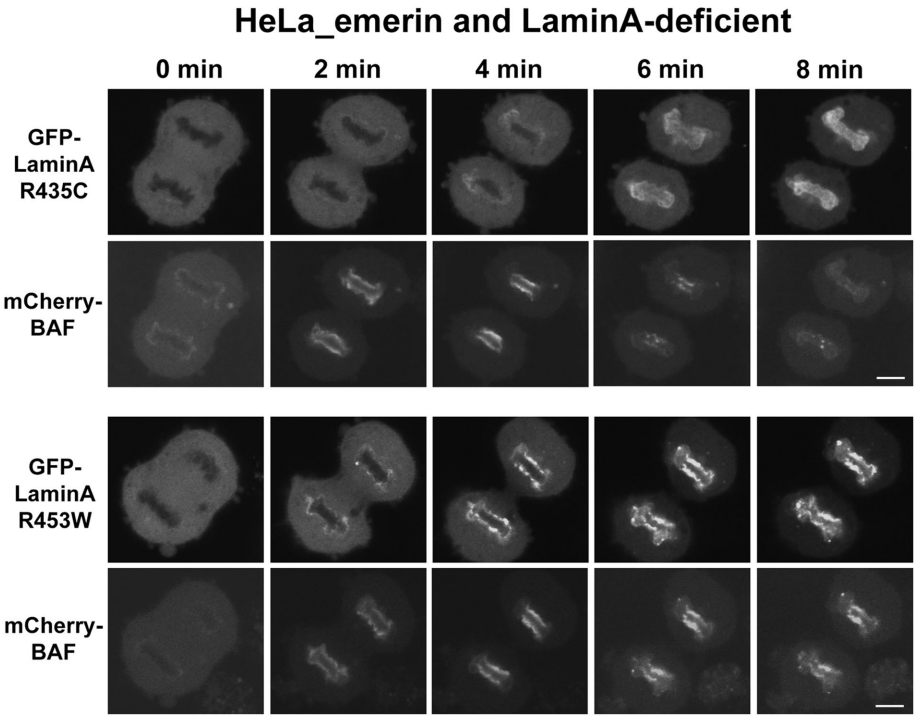

FIGURE 7: Lamin A R435C does not form aggregates on the surface of telophase chromosomes. Emerin and lamin A-double-deficient cells stably expressing mCherry-BAF were transfected with GFP-lamin A R435C (upper panels/time-lapse sequence) or GFP-lamin A R453W (lower sequence) and observed in telophase at different times after the onset of BAF reassociation with chromosomes using confocal live-cell imaging (Supplemental Video S12). Bars, 5 μm.

Next, by examining emerin and lamin A-deficient cells transfected with GFP-lamin A and mCherry-Sec61 in early telophase using confocal live-cell imaging, we observed that the first nuclear localization sites of lamin A coincided with the nascent nuclear membrane at the ends of the chromosome disks (Supplemental Figure S3B, upper panels; the arrowhead shows GFP-lamin A superimposed on the membrane labeled by mCherry-Sec61). Later in telophase, we often observed that lamin A aggregation began at the edge of the reforming nuclear membrane, where the outer membrane most likely folds into the inner nuclear membrane during progression to the inner core (Supplemental Figure S3B, lower panels, arrows; see also Supplemental Video S11, upper-left panel). The onset of lamin A aggregation at this precise location suggests a physical connection between lamin A and the nuclear membrane, as this is where lamin A would first come into contact with chromosome-bound BAF. This may indicate that part of lamin A is associated with membranes before formation of the nuclear envelope.

3. LEM and lumenal domains are necessary for targeting of emerin to the core region

We then used the possibility to correct the defect in nuclear envelope formation in emerin-deficient cells by reintroducing emerin (Figure 3) as a "rescue" assay to ask which parts of emerin are important for rapid closure of the nuclear membrane on the core region. Emerin (N-terminally tagged with mCherry) was mutated in the nucleoplasmic segment, including the LEM-domain, and in the lumenal part of the protein. Mutations are listed in Tables 1 and 2 and correspond to short deletions or to a change to alanine of a single or several amino acids. The sites (distributed throughout the entire emerin sequence) were selected on the basis of criteria such as sequence conservation, the presence of charged residues, the presence of a binding site for BAF or lamin A, involvement in X-linked EDMD, or the fact that they are located in segments proposed to mediate emerin self-interaction (Lee *et al.*, 2001; Berk *et al.*, 2014; Herrada *et al.*, 2015). Emerin mutants were transfected in emerin-deficient cells expressing GFP-BAF and cells were examined in telophase using confocal live-cell imaging. We recorded and scored for each mutant, from a total of 10 to 19 telophases per mutant, the number of cells where GFP-BAF accumulation was present at the core region 7 to 10 min after the onset of BAF binding to chromosomes (corresponding to "No Rescue" in Table 1 because the mutant did not promote nuclear envelope formation) or cells without GFP-BAF accumulation (corresponding to "Rescue"). We chose to detect the accumulation of GFP-BAF in the core region for this semiquantitative analysis because the presence or absence of this marker could be unequivocally determined for each experiment, whereas the more direct visualization of the gap in the nuclear membrane using GFP-Sec61 required that both daughter cells lie horizontally on the coverslip, which was often not the case. We also examined by time-lapse microscopy the ability of the mutants to move to and transiently concentrate at the core region. The results of these experiments are presented in Tables 1 and 2 and representative images of cells in telophase for a subset of mutants (for simplicity) are shown in Figure 8, but we also present exemplary images of all mutants in Supplemental Figures S4 and S5. First, we observed that the Mut24 mutation located in the LEM-domain, which suppresses binding to BAF (Lee *et al.*, 2001), completely prevented the rapid reconstitution of an intact nuclear membrane by emerin, implying that emerin interaction with BAF is essential for this function. In addition, the data show that the integrity of the lumenal domain of emerin was required to rescue nuclear membrane formation. Deletion of five amino acids from the C-terminus of emerin (emerinDel250) strongly affected its potential to prevent GFP-BAF accumulation at the core in emerin-deficient cells and, in this regard, the amino acids Phe254 and to a lesser extent Gly251 emerged as critical residues (Tables 1 and 2; Supplemental Figure S5). Nevertheless, quantification of the cap formed by GFP-BAF at the core region showed that BAF accumulation was less pronounced when emerin-deficient cells were transfected with mCherry-emerinDel250 than with mCherry or mCherry-emerinMut24 (Supplemental Figure S6A). Consistent with these data, emerinDel250 was enriched at the core region, but less so than full-length emerin, and emerinMut24 was not targeted to the core in telophase (Supplemental Video S14). Finally, we observed in metaphase cells that expression of emerin and emerinDel250, but not emerinMut24, induced BAF enrichment on mitotic ER membranes, presumably through binding to the LEM-domain (Supplemental Figure S6B). This indicates that emerinDel250 was located in the membrane and the LEM-domain (BAF binding site) was oriented toward the cytoplasm. These observations rule out a topological

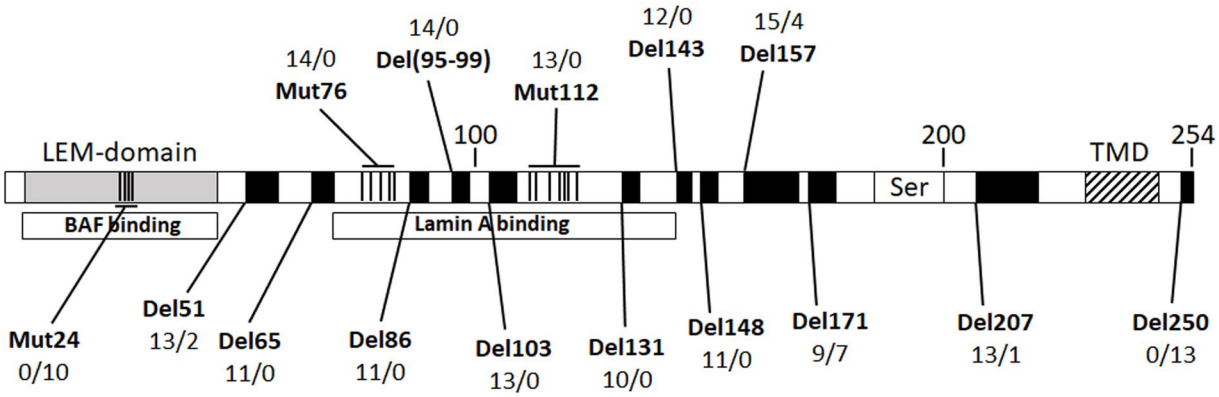

Emerin/ Mutant	Deletion/Mutation	Rescue	No Rescue	Core	Aggreg.	Property/ Function	Reference
Emerin		13	0	++			
Mut24	24GPVV →AAAA	0	10	–		BAF binding	Lee (2001)
Del51	51PSSSAASS	13	2	++			
Del65	65NSTRGD	11	0	++			
Mut76	76LPKKEDAL→ APAKADAA	14	0	++		Lamin A binding	Lee (2001)
Del86	86QSKGY	11	0	++			
Delta (95-99)	95YEESY	14	0	+[a]		EDMD mutation	Berk (2013b)
Del103	103RTYGEPE	13	0	++			
Mut112	112GPSRAVRQSVT→AASRAVAAAVA	13	0	++		Lamin A binding	Lee (2001)
Del131	131HHQVH	10	0	++			
Del143	143SEEE	12	0	++	+		
Del148	148KDRER	11	0	++	+		
Del157	157RDSAYQSITHYRP	15	4	±	++	Self-interaction[b]	Berk (2014)
Del171	171SASRSSL	9	7	±	++	Phosphorylation	Berk (2013a,b)
Del207	207RPENRAPGAGLGQD	13	1	++	+	Self-interaction[b]	Berk (2014)
Del250	250EGNPF	0	13	±	+	Lunenal domain	

Emerin-deficient HeLa cells stably expressing GFP-BAF were transiently transfected with emerin or mutated emerin fused at the N-terminus to mCherry and photographed in telophase 7 to 10 min after the onset of BAF reassociation with chromosomes using confocal live-cell imaging. In a total of 10 to 19 experiments per mutant, the number of cells that did not form a cap containing GFP-BAF at the core (Rescue) or formed a detectable cap (No Rescue) was recorded for each mutant. Exemplary images are shown in Figure 8 and Supplemental Figures S4 and S5. In addition, the ability of the mutants to target the core region (Core) was assessed in time-lapse confocal video microscopy; (++) indicates that at least three or four videos unambiguously showed robust emerin-like coalescence at the core (because the cells are not always favorably positioned to accurately see the nuclear membrane at the core region in these experiments). Finally, the propensity of the mutants to form more aggregates in the cytoplasm or in lysosomes, compared with normal emerin, was assessed visually (Aggreg.). Citations refer to the proposed property/function of the deleted or mutated region. Above Table 1: schematic representation of the deletions/mutations in emerin (254 amino acids) with corresponding scores in the rescue assay (rescue/no rescue), shown in the table. Black segments correspond to deletions and groups of black bars show mutations to alanine. "Ser" refers to a serine-rich region proximal to the trans-membrane domain (TMD) of emerin. Regions responsible for binding BAF (LEM-domain) or lamin A are indicated according to the references.

[a]Emerin Delta(95-99) was not enriched at the core like emerin.

[b]Del157 and Del207 are contained in (but do not exactly correspond to) segments proposed to mediate self-interaction in Berk (2014).

TABLE 1: Mutations in LEM-domain or in lumenal domain of emerin compromise the potential to restore nuclear membrane formation.

defect for emerinDel250 and also confirm the lack of binding of emerinMut24 to BAF.

In addition to these data, we observed that mutants in the nucleoplasmic region of emerin Del157, Del171 and to a lesser extend Del51 exhibited a decreased ability to correct the defect in nuclear membrane formation (Table 1, Figure 8, and Supplemental Figure S4). The deleted segment in emerinDel171 contains Ser173 and Ser175, which have been proposed to influence the association of emerin with BAF through phosphorylation, and the deleted segment in emerinDel157 is potentially involved in formation of an intermolecular network through emerin–emerin interaction (Hirano *et al.*, 2005; Berk *et al.*, 2013a,b; 2014). However, the most apparent consequences of these deletions were a strong tendency of the mutants to form aggregates in the cytoplasm and/or in lysosomes, a reduced localization in the nuclear envelope in interphase (assessed visually by comparison with emerin in confocal life cell imaging), as well as a reduced ability to enrich on the core region in telophase (Table 1). This suggested that the stability of these mutants was

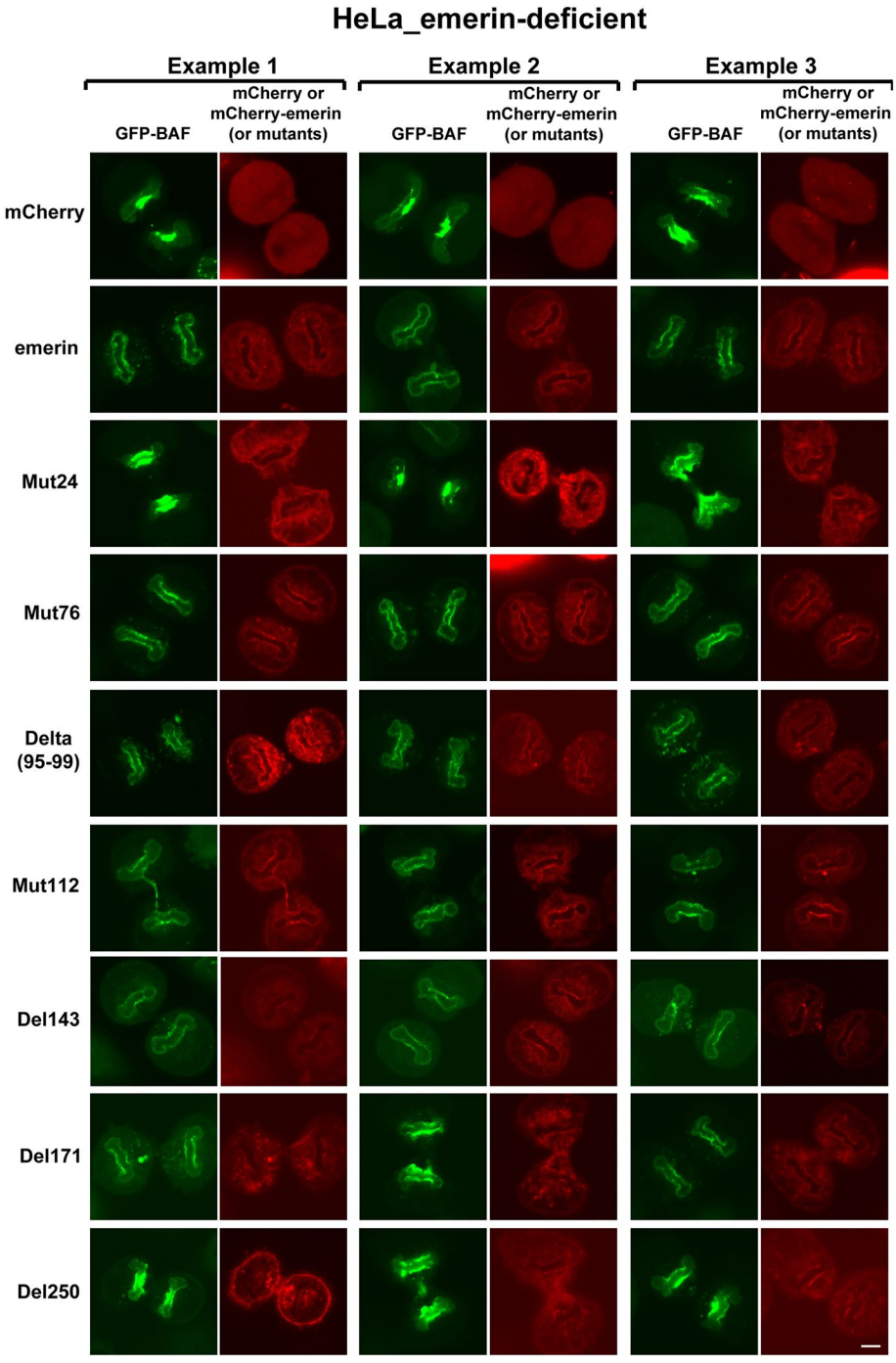

FIGURE 8: Representative images of rescue experiments using emerin mutants in emerin-deficient cells to illustrate the data in Table 1. Emerin-deficient cells stably expressing GFP-BAF transiently transfected with mCherry or mCherry fused to emerin or mutants of emerin were imaged 7 to 10 min after the onset of BAF binding to chromosomes. This figure shows a subset of the mutants described in Table 1, with three representative examples per mutant. For every example, one image (green) shows GFP-BAF and the other (red) mCherry or mCherry-emerin or mCherry-mutant of emerin. For Del171, two "rescue" and one "no rescue" (middle panel) are shown. See legend to Table 1 for a full description of the assay. Bar, 5 μm.

impaired. Emerin mutated at Ser173 and Ser175 to alanine or aspartate, individually or together, was not significantly different from normal emerin with respect to rescue or core localization (data not shown), although this does not exclude a role for phosphorylation of these residues, as aspartate might not mimic serine phosphorylation in all situations. EmerinDel51 was targeted to the core and therefore might be slightly altered in another way, for instance, due to a lack of flexibility of the LEM-domain, as it is a serine-rich segment directly adjacent to this domain.

In conclusion, the results of the mutational analysis clearly show the crucial importance of the interaction between the LEM-domain of emerin and BAF and also indicate the involvement of the lumenal domain in the cellular function/localization of emerin in telophase. Overall, the data suggest that the inability of some mutants to restore nuclear envelope reformation in emerin-deficient cells is primarily due to poor targeting to the core region, preventing emerin from performing its normal function at the nuclear envelope. Finally, it should be noted that mutants in the nucleoplasmic domain of emerin that can rescue the nuclear membrane formation might nevertheless alter the structure of the core region in telophase in ways that are difficult to distinguish at conventional microscopic resolution. This could apply, for instance, to emerin Delta(95-99), which was targeted to the core but never exhibited enrichment such as that observed for emerin (Table 1).

4. LAP2β and emerin cooperate during postmitotic nuclear envelope formation

In the final part of this study, we sought to examine the contribution of the LEM-domain protein LAP2β to the nuclear envelope formation. Similar to emerin, LAP2β has a large N-terminal nucleoplasmic region containing a LEM-domain, a single transmembrane segment, and a short C-terminal lumenal domain. Emerin and LAP2β also show some degree of sequence homology and share several binding partners (Lee *et al.*, 2001; Barton *et al.*, 2015). We used two gRNAs targeting exon 9 of the LAP2 gene (because this exon is not contained in the nucleoplasmic isoform LAP2α) to transfect emerin-deficient cells and obtained cells lacking both emerin and LAP2β (Figure 1 and Supplemental Figure S1). These double-deficient cells were stably transfected with GFP-BAF. First, we noticed in interphase a strong reduction of GFP-BAF at the nuclear rim, compared with normal HeLa cells, suggesting that emerin and LAP2β account for the majority of LEM-domain-mediated binding sites for BAF at the nuclear periphery (Supplemental Figure S2A). BAF accumulation at the core region in telophase was similar to emerin-deficient cells, but we found more cells also presenting a spot of fluorescence on the cytoplasm-facing side (Figure 9A and Supplemental Video S15). Quantification of GFP-BAF on the core region between 8 and 10 min after BAF reassociation

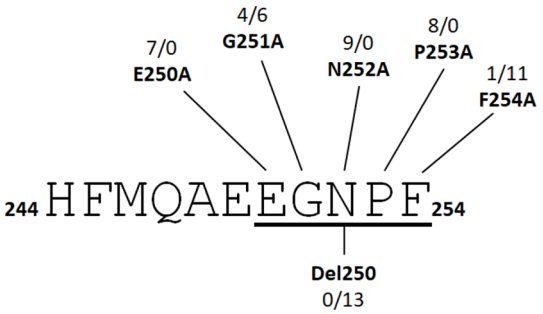

Lumenal domain mutant	Rescue	No Rescue
Del250	0	13
E250A	7	0
G251A	4	6
N252A	9	0
P253A	8	0
F254A	1	11

Emerin-deficient HeLa cells stably expressing GFP-BAF were transiently transfected with mCherry-emerin carrying the indicated amino acid substitution to alanine in the lumenal domain. They were imaged in telophase 7 min after the onset of BAF reassociation with chromosomes using confocal live-cell imaging and evaluated for their potential to rescue emerin deficiency as described in Table 1.

TABLE 2: Phe254 and Gly251 in the lumenal domain of emerin are important for restoring nuclear membrane formation.

with chromosomes shows that BAF accumulation on the cytoplasm-directed side of the core region (outer core) was increased three- to fourfold in emerin- and LAP2β-double-deficient cells compared with cells only devoid of emerin (Figure 9A). BAF was also slightly more abundant on the side facing the mitotic spindle (inner core). Depletion of LAP2β alone in HeLa cells had only a marginal impact on GFP-BAF in telophase (data not shown). Taken together, this result indicates that the defect in nuclear membrane reformation at the core region due to the absence of emerin is exacerbated when LAP2β is also depleted, suggesting that emerin and LAP2β cooperate in the last step of nuclear envelope formation. LAP2β may be sufficient most of the time in emerin-deficient cells for nuclear envelope reassembly at the outer core but not at the inner core (see *Discussion*). Consistent with these data, we observed a delay (5–10 min) in the onset of net import of NLS-GFP in telophase in both deficient cell lines compared with normal cells, which was longest for emerin- and LAP2β-deficient cells (Figure 9B). This delay likely corresponds to the period of time during which the import of NLS-GFP through functional nuclear pore complexes inserted in the nuclear membrane of the noncore region at the beginning of telophase is compensated by leakage through the unsealed membrane at the level of the core (Haraguchi *et al.*, 2008, and our observations). Thus the data in Figure 9B indicate that doubly deficient cells required the longest time to seal the nuclear membrane at the core region.

DISCUSSION

In HeLa cells, postmitotic nuclear envelope formation begins at the ends of the disk-shaped daughter nuclei, where ER cisternae associate with chromosomes. The nuclear membrane then undergoes centripetal growth/expansion toward the central part of the chromosome disk, the core region, allowing the reassembly of the nuclear envelope and insertion of nuclear pore complexes (Lu *et al.*, 2011; Tseng and Chen, 2011; LaJoie and Ullman, 2017). However, we often observed nuclear membrane segments forming on the outer core before centripetal membrane expansion was complete, suggesting that the adjacent ER may directly provide membranes to this site (see, for instance, first 2 s of Supplemental Videos S5 and S6).

We have shown in the present study that a consequence of the absence of emerin during postmitotic nuclear envelope assembly is the abnormal aggregation of lamin A on the surface of telophase chromosomes. Our data suggest that these lamin A aggregates slow down the expansion of the nuclear membrane toward the core region, ultimately inducing a local accumulation of BAF and lamin A on the uncovered region, presumably due to BAF binding to chromosomes that are exposed to the cytoplasm and to a sustained interaction between BAF and lamin A. Reintroduction of emerin in the cells prevents clustering of lamin A, restores the rapid closure of the nuclear membrane, and consequently prevents BAF accumulation on the core region.

The mutation R435C in the IgF of lamin A, which suppresses the interaction of lamin A with BAF, prevents lamin A aggregation in telophase. We conclude that lamin A clustering (and more generally targeting of lamin A to the reforming nuclear envelope) is most likely induced by IgF binding to chromosome-bound BAF and we assume that this interaction is overstabilized in the absence of emerin. Moreover, our data suggest that the part of lamin A that forms the clusters is physically connected to the reforming nuclear membrane and possibly even to mitotic ER membranes. This would explain why the aggregation of lamin A could mechanically limit nuclear membrane expansion at the surface of the chromosomes. A graphic model summarizing these conclusions is shown in Supplemental Figure S7.

At this point in the cell cycle, emerin ensures that lamin A at the periphery of the nucleus is distributed evenly in the nuclear rim, instead of being clustered around the core region. The ability of BAF to simultaneously interact with the LEM-domain of emerin and the IgF of lamin A, proposed by Samson *et al.* (2018), may allow emerin to prevent lamin A polymers from interacting (via BAF) with chromosomes for too long. In the rescue assay (Table 1), the lack of influence of mutations in the nucleoplasmic region of emerin known to abolish the direct interaction of emerin with lamin A supports a role for the tripartite complex. Emerin contained in this complex could decrease the affinity of BAF for DNA in the nuclear envelope to induce the release of lamin A from chromosomes and thus promote the rapid formation of the lamin A/C-based nuclear lamina. More speculatively, the three-part complex may induce rapid (local) rephosphorylation of BAF by a vaccinia-related kinase (VRK). For instance, VRK3 can bind and phosphorylate BAF (Park *et al.*, 2015) and, interestingly, we observed that GFP-VRK3 expressed in HeLa cells is partially enriched on the surface of the nuclei and the core region in telophase in a BAF-dependent manner (L.S., unpublished results). Likewise, VRK2A exhibits at least partial localization in the nuclear membrane, which is dependent on lamin A (Birendra *et al.*, 2017). Consistent with this possibility, phosphorylation of BAF results in a loss of affinity for DNA but does not alter binding to lamin A/C or the nucleoplasmic region of emerin (Marcelot *et al.*, 2021). Nevertheless, other mechanisms cannot be excluded and several aspects remain to be determined. For instance, an intriguing question is whether the part of lamin A that assembles at the nuclear rim in early telophase constitutes the initial postmitotic lamin A/C-based nuclear lamina, perhaps required to rapidly organize the rest of lamin A, which is then relocalized from the cytoplasm to the nucleoplasm.

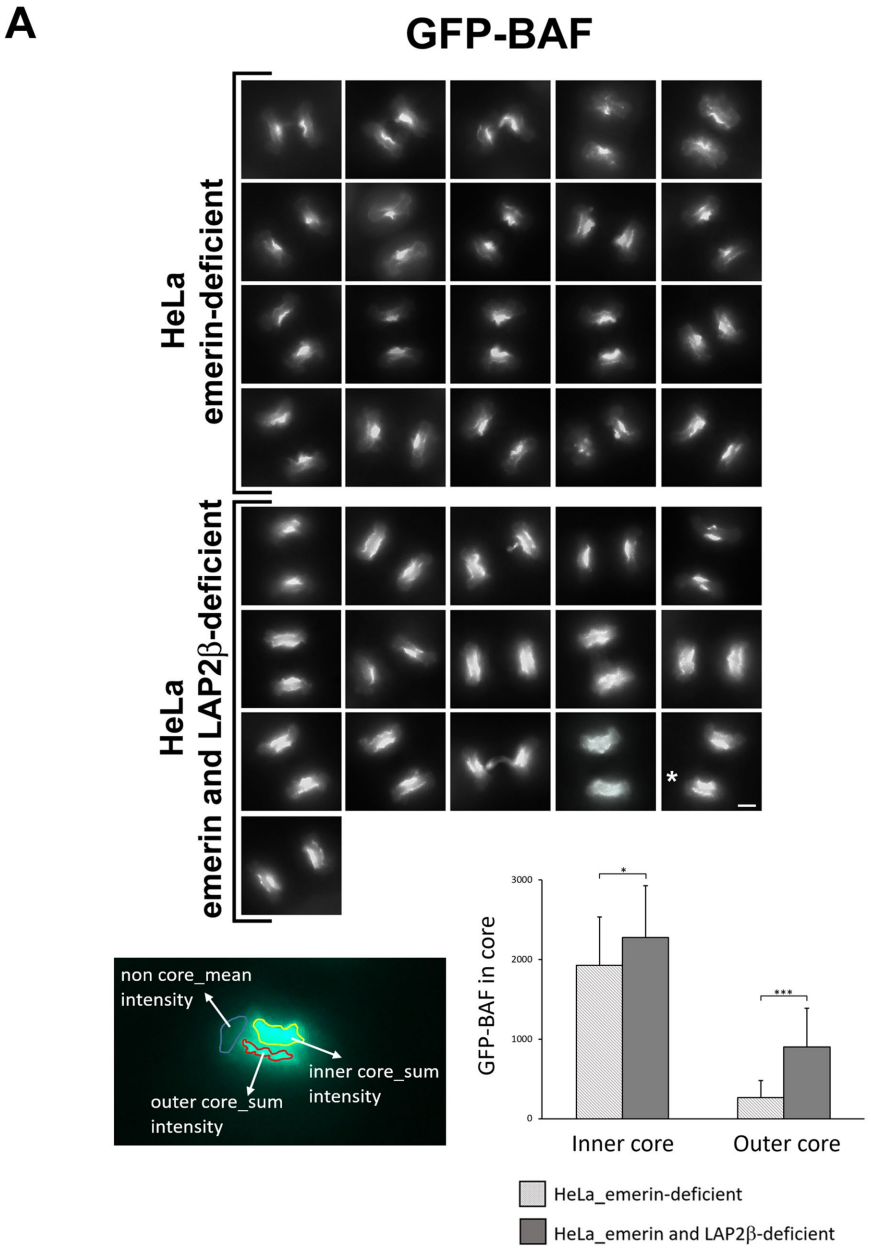

FIGURE 9: Depletion of LAP2β exacerbates the defect in nuclear membrane formation caused by emerin deficiency. (A) Twenty emerin-deficient cells and 16 emerin and LAP2β-doubly deficient cells stably expressing GFP-BAF were photographed in telophase between 8 and 10 min after the onset of BAF binding to chromosomes using epifluorescence live-cell imaging. In the graph, the sum of pixel intensities in spots corresponding to GFP-BAF accumulation at the inner or the outer core regions was divided by the mean pixel intensity in an area in the noncore region (to compensate for differences in GFP-BAF expression and/or image acquisition parameters), as illustrated in the lower-left panel (color image; the cell used for this example is indicated by an asterisk in the second last grayscale image). Results are in arbitrary units and error bars correspond to standard deviations (HeLa_emerin-deficient, hatched bars, $n = 20$, HeLa_emerin- and LAP2β-deficient, dark gray, $n = 16$). Note that cells were not transiently transfected prior to this experiment and all images were taken on the same day. Bar, 5 μm. (B) Nucleocytoplasmic ratios of NLS-GFP at different times after the onset of cytokinesis for normal, emerin-deficient or emerin- and LAP2β-deficient cells stably expressing NLS-GFP. Error bars correspond to standard deviations (HeLa, $n = 14$, HeLa_emerin-deficient, $n = 11$, HeLa_emerin- and LAP2β-deficient, $n = 9$).

The ability of mCherry-emerin to rescue the phenotype of emerin-deficient cells and the possibility to easily monitor GFP-BAF accumulation at the core region (indirectly showing the unsealed nuclear membrane at this location) were used to analyze emerin mutants and we showed that the LEM-domain (binding to BAF), the lumenal domain, and to a lesser extend a region comprising amino acids 171 to 177 are necessary for emerin function in telophase. As proposed above, it is essentially the targeting of emerin to the core region that may be affected by these mutations. Accordingly, the lumenal domain may be important for the mobility of emerin in the membrane, perhaps through specific interactions of amino acids in this domain with lipids on the lumenal side of the ER/nuclear membrane. Our data also suggest that emerin and LAP2β cooperate in nuclear membrane reformation at the core region. LAP2β could attract more membranes to the nucleus and, in most cases, compensate for the lack of emerin at the outer core, where membranes are directly supplied by the adjacent ER. LAP2β could also contribute to the resolution of lamin A aggregates but perhaps less efficiently than emerin.

The R435C mutation prevents the formation of the initial nuclear rim containing lamin A in telophase, which could affect the timing and quality of nuclear lamina reformation until interphase is established. This could have a negative influence on differentiation during tissue development, where cells divide rapidly, and contribute to pathological aspects of the progeroid syndrome restrictive dermopathy (Madej-Pilarczyk *et al.*, 2009; Youn *et al.*, 2010; Starke *et al.*, 2013). With respect to X-linked EDMD, which involves mechanisms regulating striated muscle cell maintenance and differentiation, the dependence of lamin A on emerin to organize the nuclear lamina in telophase, suggested in our study for human cells, may persist during interphase; it is known that the

structure and mechanical stability of the nuclear lamina in interphase are affected by the absence of emerin, which partly explains this disease (Muchir and Worman, 2019; Storey *et al.*, 2020). On the other hand, as discussed in the next paragraph, cells within an organism may be less affected by emerin deficiency during postmitotic nuclear envelope reformation than most cell lines in culture. This would be consistent with the absence of significant systemic effects in EDMD.

Data from previous reports and the present study help to decipher the reassembly of the postmitotic nuclear envelope. Most of cytoplasmic BAF relocalizes to chromosomes at the end of anaphase due to dephosphorylation by PP2A associated to ANKLE-2 or by other phosphatases (Haraguchi *et al.*, 2001; Asencio *et al.*, 2012; Zhuang *et al.*, 2014; Samwer *et al.*, 2017; Snyers *et al.*, 2018). The fact that the nuclear envelope begins to form at the ends of the chromosome disks in HeLa cells is most likely due to the presence of the dense mitotic spindle, which prevents direct access of membranes and components of the nuclear envelope to the core region (Lu *et al.*, 2011; Tseng and Chen, 2011; Moriuchi *et al.*, 2016). Therefore the prominent "core region" observed in HeLa cells may be a specificity of cultured/transformed cells and may be much less pronounced in cells with a normal number of chromosomes (Lu *et al.*, 2011). Then, centripetal expansion of the nuclear membrane takes place until the nuclei are completely enclosed (note that the large space to fill with nuclear membrane on the inner core in HeLa cells facilitated microscopic observations in this study). As noted above, nuclear envelope formation on the cytoplasmic side (outer core) may rely on both centripetal extension of membranes from the noncore region and direct radial input of ER-derived membrane segments from the cytoplasm, perhaps inducing the formation of several smaller "core regions." Emerin, LAP2β, and lamin A are recruited to the growing nuclear envelope and the core region by virtue of their affinity for BAF, where they move to the inner membrane to form the lamin A/C-based nuclear lamina. Since we have shown that the nuclear membrane forms in the absence of emerin and lamin A, LBR and associated proteins could provide sufficient driving force to complete postmitotic nuclear envelope formation (Tseng and Chen, 2011). Nevertheless, emerin and LAP2β most likely provide the energy needed to accelerate the final step of nuclear membrane expansion, especially at the core region. Other LEM-domain proteins are also targeted to the core region, contributing to the completion of nuclear envelope reformation. For instance, LEM2 has been shown to serve as a transmembrane ESCRT adaptor to coordinate spindle disassembly and promote nuclear membrane fusion (Gu *et al.*, 2017; von Appen *et al.*, 2020).

The reassociation of the lamins to postmitotic nuclei has been previously described. Relocalization of (nonmembrane-associated) cytoplasmic lamin A to the nucleoplasm of daughter nuclei at the end of telophase is at least partially dependent on BAF (Moir *et al.*, 2000; Haraguchi *et al.*, 2001; Moriuchi *et al.*, 2016; Snyers *et al.*, 2018). A- and B-type lamins have different modes and timing of incorporation in the nuclear lamina, as all detectable lamin B1 reassociates in a polymerized form with daughter nuclei in telophase (Moir *et al.*, 2000). In addition, lamin A and lamin B form two separate meshworks in interphase (Turgay *et al.*, 2017; Nmezi *et al.*, 2019).

Finally, it will be important to determine the exact role of BAF in the reformation of the nuclear membrane and the reassembly of the lamin A/C-based nuclear lamina after mitosis (Sears and Roux, 2020). Down-regulation of BAF using RNAi induces multilobed nuclei in telophase and it has been suggested, based on this observation, that BAF prevents the formation of micronuclei due to its DNA cross-linking property (Haraguchi *et al.*, 2008; Zhuang *et al.*, 2014; Samwer *et al.*, 2017). However, multilobed nuclei may be a consequence of incomplete depletion of BAF (as is often the case when using RNAi), resulting in a lack of coordination between BAF reassociation to chromosomes and nuclear membrane formation; therefore, complete suppression of BAF in telophase could lead to a different phenotype. In a previous study, we sometimes detected mechanical instability of telophase nuclei but not the formation of nuclear lobes or micronuclei in ANKLE2-deficient HeLa cells, although in these cells BAF does not bind to chromosomes during telophase but rather remains in the cytoplasm; furthermore, a functional nuclear membrane was formed as rapidly as in normal cells (Snyers *et al.*, 2018). Adequate cell models will help to address these intriguing questions and to better understand the interplay between BAF, LEM-domain proteins, lamin A/C, and chromosomes during reformation of the nuclear membrane and nuclear lamina after mitosis.

MATERIALS AND METHODS

Generation of cell lines using CRISPR/Cas9

HeLa or U2OS cells in 6-well plates were transfected with 1 µg of plasmid pX330 (Cong *et al.*, 2013) containing gRNAs targeting exons 1 or 2 of emerin and 60 ng of vector pEFBos.puro using Lipofectamine 2000 (Invitrogen, CA), as described (Snyers *et al.*, 2018). After selecting cells 3 d in puromycin, they were plated in 10-cm dishes and clone expansion was accomplished without antibiotics. Clones were analyzed by immunofluorescence and immunoblotting using anti-emerin mouse monoclonal antibody G-10 (sc-398067, Santa Cruz Biotechnology, Inc., TX). To produce double-deficient cells, emerin-deficient HeLa cells were transfected with targeting constructs against exon 1 of lamin A or exon 9 of LAP2. Clones were screened by immunofluorescence and immunoblotting using mouse monoclonal anti-lamin A antibody E-1 (sc-376248, Santa Cruz Biotechnology) or rabbit polyclonal anti-Thymopoietin/LAP2 antibody (NBP3-03478, NOVUS Biologicals, CO). For genomic analysis, fragments containing the targeted regions in emerin, lamin A, or LAP2 genes were amplified, subcloned in vector pGEM (Promega, WI), and sequenced. Sequences of targeting constructs and a summary of genetic modifications detected in the cell lines used in this study are presented in the Supplemental Material.

Immunoblotting

Equal amounts of proteins of total cellular extracts were separated by SDS–PAGE and transferred to a nitrocellulose membrane. Blots were blocked for 60 min in Tris-buffered saline, pH 8, containing 0.1% bovine serum albumin and 5% nonfat dry milk. After incubation with appropriate primary antibody in Tris-buffered saline, 0.1% bovine serum albumin for 45 min., they were incubated with anti-mouse or anti-rabbit alkaline phosphatase-conjugate (Sigma, USA) and visualized using NBT/BCIP. Emerin was detected with mouse monoclonal anti-emerin antibodies G-10 (sc-398067, Santa Cruz Biotechnology) and CLO 203 (NBP2-52877, Novus Biological), as shown in Figure 1 and in Supplemental Figure S1, respectively. Lamin A/C was detected with mouse monoclonal anti-lamin A/C antibodies E-1 (sc-376248, Santa Cruz Biotechnology) and WL4G10 (NBP2-59933, NOVUS Biologicals), as shown in Figure 1 and in Supplemental Figure S1, respectively. LAP2β was detected with polyclonal rabbit anti-Thymopoietin/LAP2 antibody (NBP3-03478, Novus Biologicals). Note that this antibody also recognizes the 80-kDa LAP2α isoform (Figure 1). BAF was detected using mouse monoclonal anti-BAF antibody A-11 (sc-166324, Santa Cruz Biotechnology). Rabbit antibody against GAPDH was used for the loading control (G9545, Sigma, USA).

Plasmid construction and cloning

An expression vector containing GFP-laminB receptor was a kind gift from Rey-Huei Chen, Academia Sinica, Taipei, Taiwan (Tseng and Chen, 2011). The coding regions of emerin, BAF, lamin A, and Sec61B were amplified from HeLa cell mRNA by RT-PCR and ligated in vector pCI (Promega, WI) modified to allow fusion with GFP or mCherry at the N-terminus of a protein (pCI.GFP or pCI.mCherry) or not modified. Mutagenesis of emerin and lamin A was performed by PCR using the primer extension method. For stable transfections, constructs were transferred in the vector pEFBos.puro, as described (Snyers *et al.*, 2018). All the constructs were verified by sequencing (Microsynth, Balgach, Switzerland).

Time-lapse video microscopy

For life cell imaging, cells were seeded in 6-well plates and transfected with 1 µg of plasmid DNA. The next day they were seeded on 18-mm round coverslips, which were mounted 2 d after transfection in a POCmini-2 Cell Cultivation System for microscopy (PeCon GmbH, Erbach, Germany). Time-lapse videos were recorded with a fluorescent inverted microscope Nikon Ti equipped with a 60× N.A.1.4 oil immersion lens. Video processing was done with the NIS-Elements software. For confocal life cell imaging an Olympus confocal laser scanning microscope Fluoview FV3000 equipped with a cellVivo incubation system (PeCon) was used. Confocal images and videos were processed using the cellSens software (Olympus, Japan) and final processing of videos was accomplished with the software Apowersoft (Germany). Data quantification was accomplished with NIS-Elements (Nikon) or Fiji (ImageJ) software. The program Excel was used to generate bar and line graphs and to calculate mean values and standard deviations (error bars). The number of experiments corresponding to each data point is indicated either on the graph or in the figure legend. For bar graphs, the two-sided Student's *t* test integrated in Excel was applied. *P* values were classified as ns, not significant; $*P < 0.05$; $**P < 0.01$; $***P < 0.001$.

ACKNOWLEDGMENTS

This study was in part supported by the Austrian Science Fund (FWF) Grant P30642-b28 to C.S.

REFERENCES

Asencio C, Davidson IF, Santarella-Mellwig R, Ly-Hartig TB, Mall M, Wallenfang MR, Mattaj IW, Gorjanacz M (2012). Coordination of kinase and phosphatase activities by Lem4 enables nuclear envelope reassembly during mitosis. Cell 150, 122–135.

Barton LJ, Soshnev AA, Geyer PK (2015). Networking in the nucleus: a spotlight on LEM-domain proteins. Curr Opin Cell Biol 34, 1–8.

Berk JM, Maitra S, Dawdy AW, Shabanowitz J, Hunt DF, Wilson KL (2013a). O-Linked beta-N-acetylglucosamine (O-GlcNAc) regulates emerin binding to barrier to autointegration factor (BAF) in a chromatin- and lamin B-enriched "niche." J Biol Chem 288, 30192–30209.

Berk JM, Simon DN, Jenkins-Houk CR, Westerbeck JW, Gronning-Wang LM, Carlson CR, Wilson KL (2014). The molecular basis of emerin-emerin and emerin-BAF interactions. J Cell Sci 127, 3956–3969.

Berk JM, Tifft KE, Wilson KL (2013b). The nuclear envelope LEM-domain protein emerin. Nucleus 4, 298–314.

Birendra K, May DG, Benson BV, Kim DI, Shivega WG, Ali MH, Faustino RS, Campos AR, Roux KJ (2017). VRK2A is an A-type lamin-dependent nuclear envelope kinase that phosphorylates BAF. Mol Biol Cell 28, 2241–2250.

Brachner A, Foisner R (2011). Evolvement of LEM proteins as chromatin tethers at the nuclear periphery. Biochem Soc Trans 39, 1735–1741.

Cai M, Huang Y, Ghirlando R, Wilson KL, Craigie R, Clore GM (2001). Solution structure of the constant region of nuclear envelope protein LAP2 reveals two LEM-domain structures: one binds BAF and the other binds DNA. EMBO J 20, 4399–4407.

Cong L, Ran FA, Cox D, Lin S, Barretto R, Habib N, Hsu PD, Wu X, Jiang W, Marraffini LA, *et al.* (2013). Multiplex genome engineering using CRISPR/Cas systems. Science 339, 819–823.

Dubinska-Magiera M, Koziol K, Machowska M, Piekarowicz K, Filipczak D, Rzepecki R (2019). Emerin is required for proper nucleus reassembly after mitosis: implications for new pathogenetic mechanisms for laminopathies detected in EDMD1 patients. Cells 8, 240.

Gu M, LaJoie D, Chen OS, von Appen A, Ladinsky MS, Redd MJ, Nikolova L, Bjorkman PJ, Sundquist WI, Ullman KS, *et al.* (2017). LEM2 recruits CHMP7 for ESCRT-mediated nuclear envelope closure in fission yeast and human cells. Proc Natl Acad Sci USA 114, E2166–E2175.

Guey B, Wischnewski M, Decout A, Makasheva K, Kaynak M, Sakar MS, Fierz B, Ablasser A (2020). BAF restricts cGAS on nuclear DNA to prevent innate immune activation. Science 369, 823–828.

Halfmann CT, Sears RM, Katiyar A, Busselman BW, Aman LK, Zhang Q, O'Bryan CS, Angelini TE, Lele TP, Roux KJ (2019). Repair of nuclear ruptures requires barrier-to-autointegration factor. J Cell Biol 218, 2136–2149.

Haraguchi T, Kojidani T, Koujin T, Shimi T, Osakada H, Mori C, Yamamoto A, Hiraoka Y (2008). Live cell imaging and electron microscopy reveal dynamic processes of BAF-directed nuclear envelope assembly. J Cell Sci 121, 2540–2554.

Haraguchi T, Koujin T, Hayakawa T, Kaneda T, Tsutsumi C, Imamoto N, Akazawa C, Sukegawa J, Yoneda Y, Hiraoka Y (2000). Live fluorescence imaging reveals early recruitment of emerin, LBR, RanBP2, and Nup153 to reforming functional nuclear envelopes. J Cell Sci 113, 779–794.

Haraguchi T, Koujin T, Segura-Totten M, Lee KK, Matsuoka Y, Yoneda Y, Wilson KL, Hiraoka Y (2001). BAF is required for emerin assembly into the reforming nuclear envelope. J Cell Sci 114, 4575–4585.

Herrada I, Samson C, Velours C, Renault L, Ostlund C, Chervy P, Puchkov D, Worman HJ, Buendia B, Zinn-Justin S (2015). Muscular dystrophy mutations impair the nuclear envelope emerin self-assembly properties. ACS Chem Biol 10, 2733–2742.

Hirano Y, Segawa M, Ouchi FS, Yamakawa Y, Furukawa K, Takeyasu K, Horigome T (2005). Dissociation of emerin from barrier-to-autointegration factor is regulated through mitotic phosphorylation of emerin in a xenopus egg cell-free system. J Biol Chem 280, 39925–39933.

Holaska JM, Lee KK, Kowalski AK, Wilson KL (2003). Transcriptional repressor germ cell-less (GCL) and barrier to autointegration factor (BAF) compete for binding to emerin in vitro. J Biol Chem 278, 6969–6975.

LaJoie D, Ullman KS (2017). Coordinated events of nuclear assembly. Curr Opin Cell Biol 46, 39–45.

Lee KK, Haraguchi T, Lee RS, Koujin T, Hiraoka Y, Wilson KL (2001). Distinct functional domains in emerin bind lamin A and DNA-bridging protein BAF. J Cell Sci 114, 4567–4573.

Lu L, Ladinsky MS, Kirchhausen T (2011). Formation of the postmitotic nuclear envelope from extended ER cisternae precedes nuclear pore assembly. J Cell Biol 194, 425–440.

Madej-Pilarczyk A, Rosinska-Borkowska D, Rekawek J, Marchel M, Szalus E, Jablonska S, Hausmanowa-Petrusewicz I (2009). Progeroid syndrome with scleroderma-like skin changes associated with homozygous R435C LMNA mutation. Am J Med Genet A 149A, 2387–2392.

Marcelot A, Petitalot A, Ropars V, Le Du MH, Samson C, Dubois S, Hoffmann G, Miron S, Cuniasse P, Marquez JA, *et al.* (2021). Di-phosphorylated BAF shows altered structural dynamics and binding to DNA, but interacts with its nuclear envelope partners. Nucleic Acids Res 49, 3841–3855.

Moir RD, Yoon M, Khuon S, Goldman RD (2000). Nuclear lamins A and B1: different pathways of assembly during nuclear envelope formation in living cells. J Cell Biol 151, 1155–1168.

Moriuchi T, Kuroda M, Kusumoto F, Osumi T, Hirose F (2016). Lamin A reassembly at the end of mitosis is regulated by its SUMO-interacting motif. Exp Cell Res 342, 83–94.

Muchir A, Worman HJ (2019). Emery-Dreifuss muscular dystrophy: focal point nuclear envelope. Curr Opin Neurol 32, 728–734.

Nmezi B, Xu J, Fu R, Armiger TJ, Rodriguez-Bey G, Powell JS, Ma H, Sullivan M, Tu Y, Chen NY, *et al.* (2019). Concentric organization of A- and B-type lamins predicts their distinct roles in the spatial organization and stability of the nuclear lamina. Proc Natl Acad Sci USA 116, 4307–4315.

Park CH, Ryu HG, Kim SH, Lee D, Song H, Kim KT (2015). Presumed pseudokinase VRK3 functions as a BAF kinase. Biochim Biophys Acta 1853, 1738–1748.

Samson C, Celli F, Hendriks K, Zinke M, Essawy N, Herrada I, Arteni AA, Theillet FX, Alpha-Bazin B, Armengaud J, *et al.* (2017). Emerin self-assembly mechanism: role of the LEM domain. FEBS J 284, 338–352.

Samson C, Petitalot A, Celli F, Herrada I, Ropars V, Le Du MH, Nhiri N, Jacquet E, Arteni AA, Buendia B, *et al.* (2018). Structural analysis of the ternary complex between lamin A/C, BAF and emerin identifies an interface disrupted in autosomal recessive progeroid diseases. Nucleic Acids Res 46, 10460–10473.

Samwer M, Schneider MWG, Hoefler R, Schmalhorst PS, Jude JG, Zuber J, Gerlich DW (2017). DNA cross-bridging shapes a single nucleus from a set of mitotic chromosomes. Cell 170, 956–972.e923.

Sears RM, Roux KJ (2020). Diverse cellular functions of barrier-to-autointegration factor and its roles in disease. J Cell Sci 133, jcs246546.

Snyers L, Erhart R, Laffer S, Pusch O, Weipoltshammer K, Schofer C (2018). LEM4/ANKLE-2 deficiency impairs post-mitotic re-localization of BAF, LAP2alpha and LaminA to the nucleus, causes nuclear envelope instability in telophase and leads to hyperploidy in HeLa cells. Eur J Cell Biol 97, 63–74.

Starke S, Meinke P, Camozzi D, Mattioli E, Pfaeffle R, Siekmeyer M, Hirsch W, Horn LC, Paasch U, Mitter D, *et al.* (2013). Progeroid laminopathy with restrictive dermopathy-like features caused by an isodisomic LMNA mutation p.R435C. Aging (Albany NY) 5, 445–459.

Storey EC, Holt I, Morris GE, Fuller HR (2020). Muscle cell differentiation and development pathway defects in Emery-Dreifuss muscular dystrophy. Neuromuscul Disord 30, 443–456.

Tseng LC, Chen RH (2011). Temporal control of nuclear envelope assembly by phosphorylation of lamin B receptor. Mol Biol Cell 22, 3306–3317.

Turgay Y, Eibauer M, Goldman AE, Shimi T, Khayat M, Ben-Harush K, Dubrovsky-Gaupp A, Sapra KT, Goldman RD, Medalia O (2017). The molecular architecture of lamins in somatic cells. Nature 543, 261–264.

von Appen A, LaJoie D, Johnson IE, Trnka MJ, Pick SM, Burlingame AL, Ullman KS, Frost A (2020). LEM2 phase separation promotes ESCRT-mediated nuclear envelope reformation. Nature 582, 115–118.

Wiebe MS, Jamin A (2016). The barrier to autointegration factor: interlocking antiviral defense with genome maintenance. J Virol 90, 3806–3809.

Youn GJ, Uzunyan M, Vachon L, Johnson J, Winder TL, Yano S (2010). Autosomal recessive LMNA mutation causing restrictive dermopathy. Clin Genet 78, 199–200.

Young AM, Gunn AL, Hatch EM (2020). BAF facilitates interphase nuclear membrane repair through recruitment of nuclear transmembrane proteins. Mol Biol Cell 31, 1551–1560.

Yuan J, Xue B (2015). Role of structural flexibility in the evolution of emerin. J Theor Biol 385, 102–111.

Zhuang X, Semenova E, Maric D, Craigie R (2014). Dephosphorylation of barrier-to-autointegration factor by protein phosphatase 4 and its role in cell mitosis. J Biol Chem 289, 1119–1127.